

Effect of expanded perlite aggregates and temperature on the strength and dynamic elastic properties of cement mortar

Sergiu-Mihai Alexa-Stratulat, George Taranu, Ana-Maria Toma*, Ioana Olteanu, Cristian Pastia, Georgiana Bunea, Ionut-Ovidiu Toma*

The "Gheorghe Asachi" Technical University of Iasi, Faculty of Civil Engineering and Building Services, Iasi, Romania



ARTICLE INFO

Keywords:

Expanded perlite aggregate mortar
Dynamic modulus of elasticity
Flexural strength
Compressive strength
Elevated temperature

ABSTRACT

The residential market consumes nearly half of the world's concrete production, and it is anticipated that 68 % of the global population will reside in urban areas by 2050. Researchers have focused their efforts on exploring alternative options to natural aggregates in concrete and mortar. In line with the principles of circular economy, construction and demolition waste has been repurposed for the manufacture of cement-based materials. Volcanic products, which are abundant but underutilized, have been identified as an alternative to recycled aggregates. They offer several advantages over natural river aggregates, including reduced weight, enhanced thermal and acoustic insulation, improved fire resistance and pozzolanic characteristics. While there has been a significant amount of research on the use of expanded perlite as a supplementary cementitious material, studies involving the use of expanded perlite aggregates (EPA) in cement-based construction materials are relatively limited. This paper seeks to address this knowledge gap by investigating the use of EPA in cement-based mortar at both room and elevated temperatures. The study examines the impact of varying replacement percentages (10 %, 20 % and 30 % - by volume) of natural sand with EPA having a maximum grain size of 4 mm, and the exposure temperature of mortar prisms at the age of 28 days. Specifically, temperatures of 100°C, 150°C and 200°C were selected for analysis. The impact of these parameters on the flexural and compressive strength of mortar, as well as its dynamic elastic properties, was experimentally determined. The findings indicate that, at room temperature, higher replacement percentages of natural sand by EPA result in decreased flexural and compressive strengths, by as much as 50 % and 30.71 %, respectively. However, the dynamic moduli values for replacement percentages up to 20 % are similar to those of the reference mix. Conversely, when subjected to temperatures up to 200°C, significant improvements were observed in the flexural strength values, e.g. over 20 % for temperatures of 150°C and 200°C, with only marginal improvements in compressive strength, 3 % ÷ 20 % for temperatures of 150°C and 200°C, compared to values obtained at room temperature.

1. Introduction

Concrete is the most widely used construction material with a total worldwide production of 14 billion cubic meters in 2020, according to Global Cement and Concrete Association [1]. Nearly half of this quantity served the residential sector. Projections indicate that 68 % of the world's population will inhabit urban areas by 2050, leading to an estimated annual concrete production of 20 billion cubic meters. Given that aggregates constitute 60 %-75 % of the total concrete volume, it follows that the demand for natural resources will increase substantially.

It is estimated that approximately 50 % of the world's raw material consumption is necessary to sustain this demand [2].

Finding alternative solutions to natural aggregates has been actively pursued by many researchers. The use of ferrochrome waste slag aggregates in limestone-calcined clay cement mortar resulted in an increase in both tensile strength (up to 22.2 %) and compressive strength (up to 71 %), as the percentage of natural sand replacement increased [3]. In addition, when natural sand was completely replaced with ferrochrome waste slag aggregates, the water absorption coefficient decreased by 16 %. In line with the principles of circular economy,

* Corresponding authors.

E-mail addresses: sergiu-mihai.alex Stratulat@academic.tuiasi.ro (S.-M. Alexa-Stratulat), george.taranu@academic.tuiasi.ro (G. Taranu), ana-maria.toma@academic.tuiasi.ro (A.-M. Toma), ioana.olteanu@academic.tuiasi.ro (I. Olteanu), cristian.pastia@academic.tuiasi.ro (C. Pastia), georgiana.bunea@academic.tuiasi.ro (G. Bunea), ionut.ovidiu.toma@tuiasi.ro (I.-O. Toma).

construction and demolition waste has been repurposed as a resource for cement-based materials production. A recent study used recycled aggregates to substitute natural sand in mortar at rates of 25 %, 50 %, 75 %, and 100 %. Apart from demonstrating their effectiveness in structural applications, such as masonry elements, completely replacing natural with recycled aggregates with particle size smaller than 2.4 mm resulted in a 64 % reduction of CO₂ emissions associated with production processes. However, after considering both the strength properties and carbon footprint, it was concluded that optimal replacement percentage was 50 % [2].

The use of recycled aggregates from construction and demolition waste in concrete typically results in a decrease in mechanical properties. This is primarily attributed to the quality of the aggregates, which weakens the interfacial transition zone between the porous mortar adhering to the surface of the recycled aggregates and the fresh cement paste [4,5]. A possible solution to this issue involves treating the recycled aggregates with a silica fume slurry. This yielded a notable 16 %-26 % increase in concrete compressive strength at various curing ages, with complete replacement of natural aggregates. The inclusion of carbon fibers resulted in a 38 % increase in the flexural strength of concrete with recycled aggregates and a 34 % increase in the modulus of elasticity [6]. In a separate study, different combinations of recycled aggregates and nano-silica were examined to assess their impact on the mechanical and durability properties of concrete. Researchers employed gene expression programming to predict the compressive strength of concrete incorporating recycled aggregates and nano-silica as a pozzolan [7]. The proposed optimal mix comprised a 26 % replacement of natural coarse aggregates with recycled aggregates and 4 % nano-silica. According to the mathematical model, this mix demonstrated the highest flexural and compressive strength, modulus of elasticity and, simultaneously, the lowest water absorption coefficient.

An alternative to recycled aggregates has been identified in the form of volcanic products, which, despite their substantial potential, are not fully exploited. Volcanic rocks such as pumice, lapillus, tuff, zeolites, and perlite offer several advantages over natural river aggregates, including their lightweight nature, improved thermal and acoustic insulation properties, fire resistance, and pozzolanic properties [8]. The use of volcanic scoria, a type of volcanic rock formed by rapid cooling of lava in air, in concrete led to a 15 % reduction of bulk density and a 22.3 % increase in modulus of elasticity. Furthermore, due to secondary pozzolanic reactions, the compressive strength increased between 28 and 90 days by 15.23 %-22.3 %. However, the obtained values were approximately 70 %-75 % of the compressive strength obtained for the

reference mix [9]. The use of zeolites as lightweight aggregates in concrete proved to be advantageous from the point of view of self-weight reduction. Additionally, a smaller interfacial transition zone between the aggregates and the cement paste was achieved, depending on the type of cement used in the concrete mix [10]. High quantities of ettringite and calcium hydroxide (CH) at early ages, and correspondingly high levels of calcium silicate hydrates (CSH) at later ages, were identified as the main factors influencing the quality of the interfacial transition zone, with a pronounced dependence on cement dosage and water-to-cement ratio.

Perlite, an amorphous aluminosilicate volcanic glass, has the ability to expand approximately 5–20 times its original volume when heated to its softening temperature, ranging between 900°C and 1200°C [11]. This expansion process, caused by the water trapped inside the perlite ore, results in a lightweight, cellular aggregate with bulk densities ranging from 80 kg/m³ to 240 kg/m³ [12]. Expanded perlite, with its high surface area, low sound transmission, low thermal conductivity [12,13] and chemical inertness, finds a wide range of applications, from horticulture to pharmaceutical and filtering applications in municipal drainage systems. In the construction industry, it has been used as a replacement for cement [14] and/or aggregates [11]. Taking into account the many applications of perlite, its worldwide production steadily increased during the last decade, as shown in Fig. 1.

One of the earliest uses of perlite in the construction industry has been in the development of building insulation materials, such as renders and mortars. Considering that approximately 40 % of a building's total energy consumption is dedicated to maintaining a comfortable indoor climate [12,16], there has been a growing demand for improved insulating materials and more efficient cooling and heating systems. Laboratory investigations and numerical analyses have demonstrated that panels composed of a mixture of cement, expanded perlite and pumice exhibit superior thermal performance in both standard (no vegetation) and green roof scenarios compared to reference panels [12]. Combining perlite powder with a sodium hydroxide solution and a foaming agent result in an ultra-lightweight foam concrete-like material, with enhanced thermal properties and fire performance. Heat treatment, particularly at a curing temperature of 850°C, was identified as an important parameter, yielding the best results in terms of density and thermal conductivity [13]. Additionally, owing to the pozzolanic activity of perlite, a denser and stronger structure of renders and mortars is obtained [17]. A similar densification effect has been observed in the case of a magnesium potassium phosphate cement-expanded perlite composite, used as a fire-resistant coating. The presence of perlite

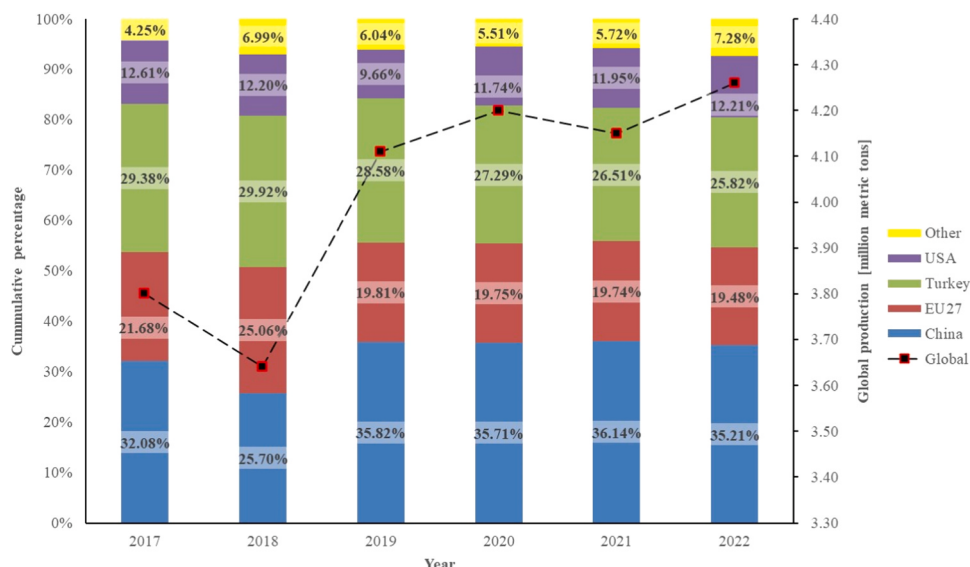


Fig. 1. Worldwide perlite ore production (based on data from USGS [15]).

increased residual bond strength after the fire test and reduced the occurrence of visible cracks on the coating surface [18].

The production of cement is a significant contributor to greenhouse gas (GHG) emissions in the construction industry, accounting for approximately 5 % - 7 % of the global CO₂ emissions [19,20]. To address this environmental impact, the use of supplementary cementitious materials (SCMs) has been proposed as a feasible solution. SCMs can be classified based on their source into industrial wastes, such as silica fume and fly ash, and natural pozzolans, such as pumice, metakaolin, perlite, zeolite and others. Natural pozzolans are aluminosilicate materials capable of reacting with calcium hydroxide (CH) to form calcium silicate hydrates (CSH) gels, contributing to a denser structure in cementitious materials and enhancing strength and durability properties [21]. Research has shown that using perlite powder in self-compacting concrete (SCC) requires an increase in superplasticizer content to achieve similar workability to the reference mix. Compressive strength values were found to be nearly identical to the reference mix at the age of 91 days, with significant improvements observed with increasing the fineness of perlite powder from the age of 28 days [22]. The use of perlite powder in SCC resulted in improved mechanical properties when exposed elevated temperatures, up to 600°C, with reduced spalling [23]. Replacing cement with high percentages of perlite powder, such as 20 % and 30 %, had a detrimental effect on concrete protection of reinforcement to corrosion in aggressive environments [24]. However, a 40 % replacement of cement by expanded perlite powder yielded comparable 28-day compressive strength values in ultra-high performance concrete (UHPC) but slightly reduced the chloride ion penetration resistance of concrete [25].

In an effort to prevent the depletion of natural resources used in concrete production, researchers have explored alternatives to conventional aggregates. Other forms of natural aggregates, such as expanded perlite, zeolites, and volcanic tuff, were identified, and their impact on the mechanical properties of concrete were evaluated. A recent study focused on the replacement of coarse natural aggregates with perlite aggregates concluded that concrete density is significantly reduced due to perlite porous structure [26]. However, as perlite possesses lower strength than traditional aggregates, the compressive strength of concrete decreased with increasing replacement percentage. Conversely, concrete with expanded perlite aggregates (EPA) demonstrated higher compressive strength values at both 7 and 28 days compared to other lightweight concrete mixes based on pumice aggregates [27]. Moreover, replacing natural sand with EPA in proportions of 75 %–100 % resulted in obtaining ultra-high performance concrete with similar fluidity, mechanical strength and durability properties as conventional UHPC [25].

The existing scientific literature contains a significantly higher number of studies dedicated to perlite as a supplementary cementitious material compared to those investigating expanded perlite as an aggregate substitute. This paper seeks to address this knowledge gap by investigating the use of EPA in cement-based mortar at both room temperature and after exposure to elevated temperatures. Previous research has shown that concrete incorporating powdered perlite exhibited enhanced mechanical properties at temperatures up to 300°C [23,28]. Therefore, this study focused on evaluating the impact of replacing natural sand with EPA, with a maximum grain size of 4 mm, at varying percentages (10 %, 20 % and 30 % by volume) as well as subjecting mortar prisms to temperature exposure at 28 days. The temperatures selected for the experiment were 100°C, 150°C and 200°C. Experimental determinations were made regarding the impact of both parameters on the flexural and compressive strength of mortar, and on its dynamic elastic properties.

The results indicate that, at room temperature, an increase in replacement percentage of natural sand with EPA leads to decreased flexural strength and compressive strength. However, replacement percentages of up to 20 % exhibit dynamic moduli values similar to those of the reference mix. Conversely, when exposed to temperatures up to 200°C, there are significant improvements in the flexural strength

and minimal gains in compressive strength, compared to the values obtained at room temperature. The most substantial increases were observed at 150°C.

2. Materials and methods

2.1. Materials

A CEM II B-M (S-L) 42.5 R cement (StructoPlus), complying with SR EN 197-1:2011 [29] guidelines, was considered in this research. It is widely available on the market, and it comprises 65 %–79 % clinker and a 21 %–35 % combination of blast furnace slag and limestone. The chemical composition of the cement, as provided by the manufacturer (HOLCIM, Romania), is detailed in Table 1. According to Favier et al. [30], CEM II cement is the predominant type in Europe, holding a 47 % market share in 2015.

The aggregate used in this study was river sand with a maximum grain size of 4 mm and a specific weight of 2.69. Expanded perlite, having a specific weight of 0.129 and complying to SR EN 1097-3:2002 [31] and SR EN 933-2:2020 [32], was selected as a substitute for the natural sand, with replacement volumes of 10 %, 20 % and 30 %. Table 1 provides the chemical composition of the expanded perlite, as supplied by the manufacturer (ProcemaPerlit). The sieve analysis of the two types of aggregates is presented in Fig. 2. It can be observed that EPA had almost 60 % of its volume consisting of grains larger than 1 mm [33], whereas in case of sand the percentage was significantly lower, 18.16 %. However, since EPA aggregates have a lower Mohs hardness compared to natural sand, it is expected that particle size distribution of EPA will change during mixing, namely the volume of fine grains to increase, as previously reported [33]. The percentage shown in Fig. 3 for 0.125 mm sieve corresponded to even lower than 0.063 mm sieve, which basically falls in the category of powders. In case of sand, the corresponding percentage was only 3.4 %.

Based on the specifications provided by ASTM C618:2022 [34], expanded perlite falls in the category of natural pozzolans due to the combined content of SiO₂, Al₂O₃ and Fe₂O₃ exceeding 70 % [35]. Fig. 3a depicts the porous structure of expanded perlite. When further magnified, the microstructure shows a series of flakes/sheets [36] separated by gaps, as shown in Fig. 3b. These features contribute to the thermal insulation and water absorption properties of expanded perlite [37].

2.2. Mix proportion

A reference mortar mix ratio of 1:4:0.6 (cement:sand:water) by volume was employed. Table 2 shows the proportions, per cubic meter, for all mixes used in the study. For mortars modified by EPA, a higher water/cement ratio was required to achieve a consistency similar to that of the reference mix [14]. In other previous studies, superplasticizer was used in order to keep the same water/cement ratio [33]. However, according to earlier findings, there are large compatibility issues between various superplasticizers and natural pozzolans [38]. For similar water/binder ratio it was found that there is a need to increase the superplasticizer content by as much as 50 % to counteract the loss of slump caused by the use of zeolite (having similar chemical composition to perlite). Moreover, different superplasticizers required different dosages in order to achieve similar workability of mortar.

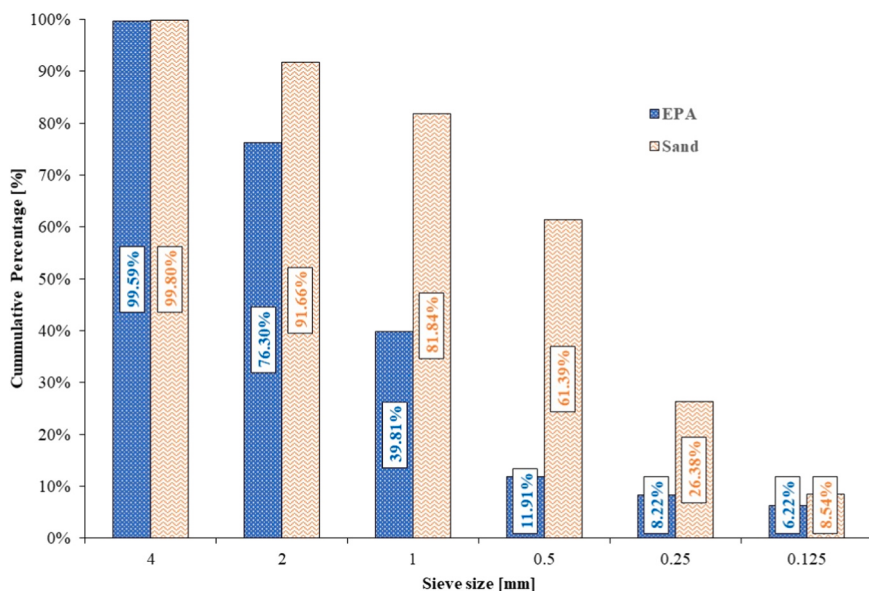
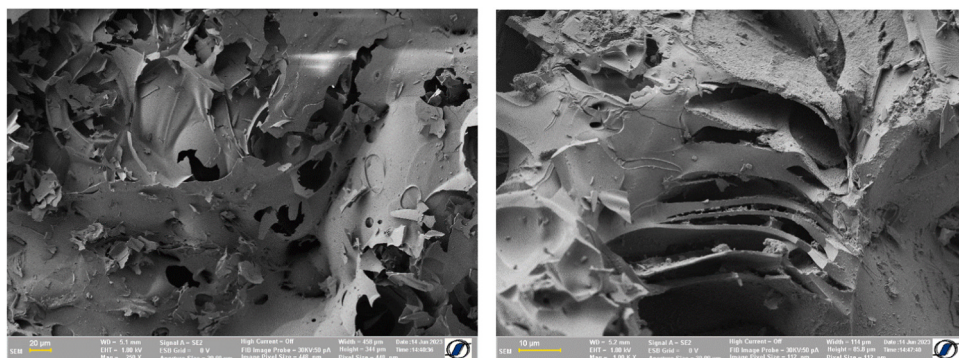
Aside of the reference, the mixtures were labeled by EPA (expanded perlite aggregate) and a number indicating the percentage of sand replacement. For each mix outlined in Table 2, twelve standard prisms, each measuring 40 mm × 40 mm × 160 mm in height, width, and length respectively [39], were cast. This resulted in a total of 48 specimens. The prismatic steel molds were mounted on a jolting table (drop height of 15 mm) and vibrated in accordance with specifications of SR EN 196-1:2016 [39]. After vibration, there was no bleeding water visible on the surface of the mortar prisms.

The mortar prisms were demolded after 24 hours from casting and

Table 1

Chemical composition of CEM II cement and expanded perlite (expressed in %).

	CaO	SiO ₂	Al ₂ O ₃	Fe ₂ O ₃	MgO	SO ₃	Na ₂ O	K ₂ O	Cl
CEM II	58.49	16.32	4.83	2.24	1.39	2.85	0.34	0.46	0.035
CaO		SiO ₂	Al ₂ O ₃	Fe ₂ O ₃	MgO	SO ₃	Na ₂ O+K ₂ O		Cl
Expanded Perlite	1.3–1.7	74–77	12–15	1.1–1.6	0.1–0.7	-	5.0–8.0		-

**Fig. 2.** Sieve analysis of EPA and natural sand.**a)** porous structure**b)** flake-like microstructure**Fig. 3.** SEM images of expanded perlite.**Table 2**

Mix proportions of mortars used in this study.

Mix designation	Cement [kg/m ³]	Sand [kg/m ³]	EPA [kg/m ³]	Water / Cement
Ref	380	1550	-	0.60
EPA10		1395	7.42	0.65
EPA20		1240	14.85	
EPA30		1085	22.28	

stored in water at 22°C±1°C for 27 days, until the day of testing. Prior to storing the mortar prisms in water, their geometrical dimensions were measured, as presented in Section 2.3.2, to check for compatibility with the dimensions of the steel mold. Additionally, there were no large voids on the surface of the mortar prisms, suggesting that the mortar fully filled the steel mold.

2.3. Methods

2.3.1. Slump test

The slump was assessed using a mini-slump test with a cone of dimensions 100 mm×70 mm×60 mm (bottom diameter × top diameter × height) [40,41]. Once the cone was lifted and the spread of the mortar ceased, the average of three measured diameters was taken into account. In addition, the height reduction was measured relative to the height of the cone.

2.3.2. Dimensions and mass

At the age of 28 days, the mortar prisms were taken out of the water, wiped clean with a thick cloth to remove the excess of water. Afterwards, they were weighed, using a digital scale with an accuracy of 0.01 g, and then measured with the digital caliper, accuracy of 0.01 mm, to check for dimensional stability and also to be able to compute the bulk

density of the obtained mortars. Measurements were recorded for both length (four values) and width/height (six values) of the prisms.

2.3.3. Dynamic moduli of elasticity

The dynamic moduli of elasticity were determined in accordance with ASTM C215:19 specifications [42]. The determination of longitudinal dynamic modulus of elasticity and dynamic shear modulus were based on the first resonant frequencies in longitudinal and transversal directions, respectively, obtained by means of Impact Echo Method (Fig. 4).

The dynamic longitudinal modulus of elasticity was calculated on the basis of Eq. 1 [42]:

$$E_{dyn} = D \cdot M \cdot (n')^2 \quad (1)$$

where: M is the mass of specimen (kg), n' is the fundamental longitudinal frequency of vibration (Hz) and $D = \frac{4 \cdot L}{b \cdot t}$ is a coefficient ($\frac{N \cdot s^2}{kg \cdot m^2}$) that depends on the length L (m) and the cross sectional dimensions b (m) and t (m) of the specimen.

The dynamic shear modulus was calculated using Eq. 2 [42]:

$$G_{dyn} = B \cdot M \cdot (n'')^2 \quad (2)$$

where: M is the mass of specimen (kg), n'' is the fundamental torsional frequency of vibration (Hz) and $B = \frac{4 \cdot L \cdot R}{A}$ is a coefficient ($\frac{N \cdot s^2}{kg \cdot m^2}$) that depends on the length L (m), of the specimen the cross-sectional area A (m^2) and the shape factor R which takes the value of 1.183 for a square cross-section prism [42].

The experimental arrangement depicted in Fig. 4a was used to record the longitudinal free vibration response of all specimens. The signal for each prism consisted of at least 10 impact responses, as exemplified in Fig. 5a for the Ref mix. This signal underwent the Fast Fourier Transform (FFT) analysis, and the frequency spectrum was obtained (Fig. 5b). The fundamental longitudinal frequency was identified by applying a Pseudo-Voigt fitting function on the FFT spectrum (Fig. 5c). The dynamic modulus of elasticity was calculated using Eq. 1.

A similar method was applied to obtain the torsional vibration frequency, employing the set-up outlined in Fig. 4b. Upon obtaining the FFT spectra, two main peaks, closely positioned, were observed, as depicted in Fig. 6a for the Ref mix. Consequently, the fundamental transversal frequency of vibration was also measured, employing the set-up presented in Fig. 4c. This frequency was then neglected in the analysis of the torsional response, which was fitted with the same Pseudo-Voigt function (Fig. 6b). The fundamental torsional frequency was then used to compute the dynamic shear modulus of each prism using Eq. 2.

The dynamic Poisson ratio was computed by means of Eq. 3:

$$\nu_{dyn} = \frac{E_{dyn}}{2G_{dyn}} - 1 \quad (3)$$

where E_{dyn} is the dynamic modulus of elasticity and G_{dyn} is the dynamic shear modulus determined based on Eqs. (1) and (2), respectively.

2.3.4. Temperature

Cement-based materials, such as mortar, concrete and reinforced concrete, may be exposed to severe environmental conditions, including high temperatures. Under extreme circumstances, fire incidents may occur either due to natural disasters or human error. Exposure to high temperatures triggers a series of internal changes in the material that negatively impact its mechanical properties. Previous research indicates that the cement paste is the most vulnerable component or mortar or concrete to high temperatures [43,44]. When exposed to temperatures higher than 900°C the cement paste loses 80 % of its strength [45]. The initial effect is the loss of free and capillary water, with the evaporation process starting at approximately 100°C. However, given the pore pressure inside the cement-based material, this process takes place within the 100°C-140°C temperature range [46]. While the loss of water may lead to shrinkage in the cement paste, its impact on the dimensional stability of elements is generally counteracted by the expansion of non-hydrated products, such as un-hydrated cement grains and calcium hydroxide [47].

The dehydration of ettringite occurs between 80°C and 150°C, while the decomposition of gypsum takes place at 150°C-170°C. The dehydration process of calcium silicate hydrate (CSH) initiates around 200°C [48]. Previous studies indicated that cement-based materials do not experience substantial strength reduction when exposed to temperatures up to 300°C. Any strength loss that occurs is reversible, due to the rehydration process occurring during and after the cooling phase [49].

The selection of temperature values was based on previously mentioned studies on concrete, coupled with the findings of Castellote et al. [50] on cement pastes. Considering the information presented above, the temperature thresholds chosen for this study were 100°C (marking the onset of evaporation of free and capillary water), 150°C (indicating the end of free and capillary water evaporation, as well as the dehydration of ettringite) and 200°C (concluding gypsum decomposition and the beginning of CSH dehydration, but still well below 300°C). For the purpose of this study, the prisms were placed in an oven, heated to the target temperature, and maintained at that temperature for 4 hours. Once the heating process was terminated, the prisms were allowed to cool gradually to room temperature inside the oven at a cooling rate of 0.5 °C/min. The temperature increase rate was consistent for all specimens, at 6°C per minute, as shown in Fig. 7.

After being exposed to elevated temperature, the specimens were measured to check for any changes in the geometrical dimensions and weighted to account for the mass loss due to evaporation processes. The dynamic elastic properties were determined following the procedure outlined in Section 2.3.3.

2.3.5. Flexural-tensile strength and compressive strength

The flexural tensile strength and compressive strength of all mortar prisms were assessed in compliance with SR EN 196-1:2016 [39]. Three-point bending test, with a loading rate of 50 N/s, was used to determine the flexural tensile strength. The resulting broken parts of the prism were examined for signs of visible cracks and then subjected to uniaxial compression test with a loading rate of 2400 N/s.

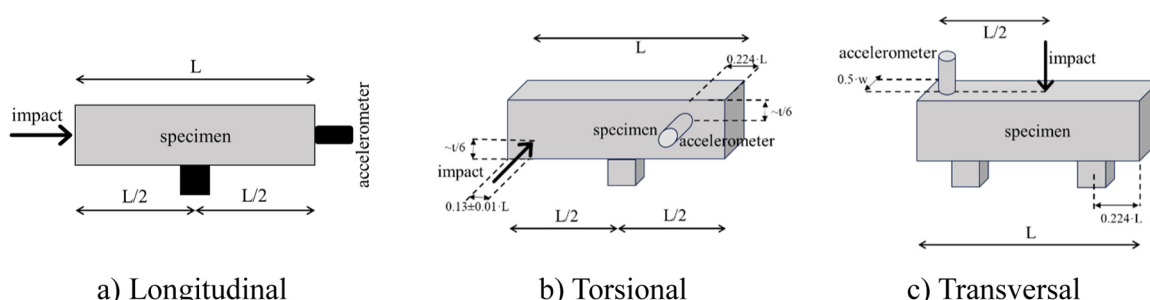


Fig. 4. Set-up for determination of fundamental frequency of vibration [42].

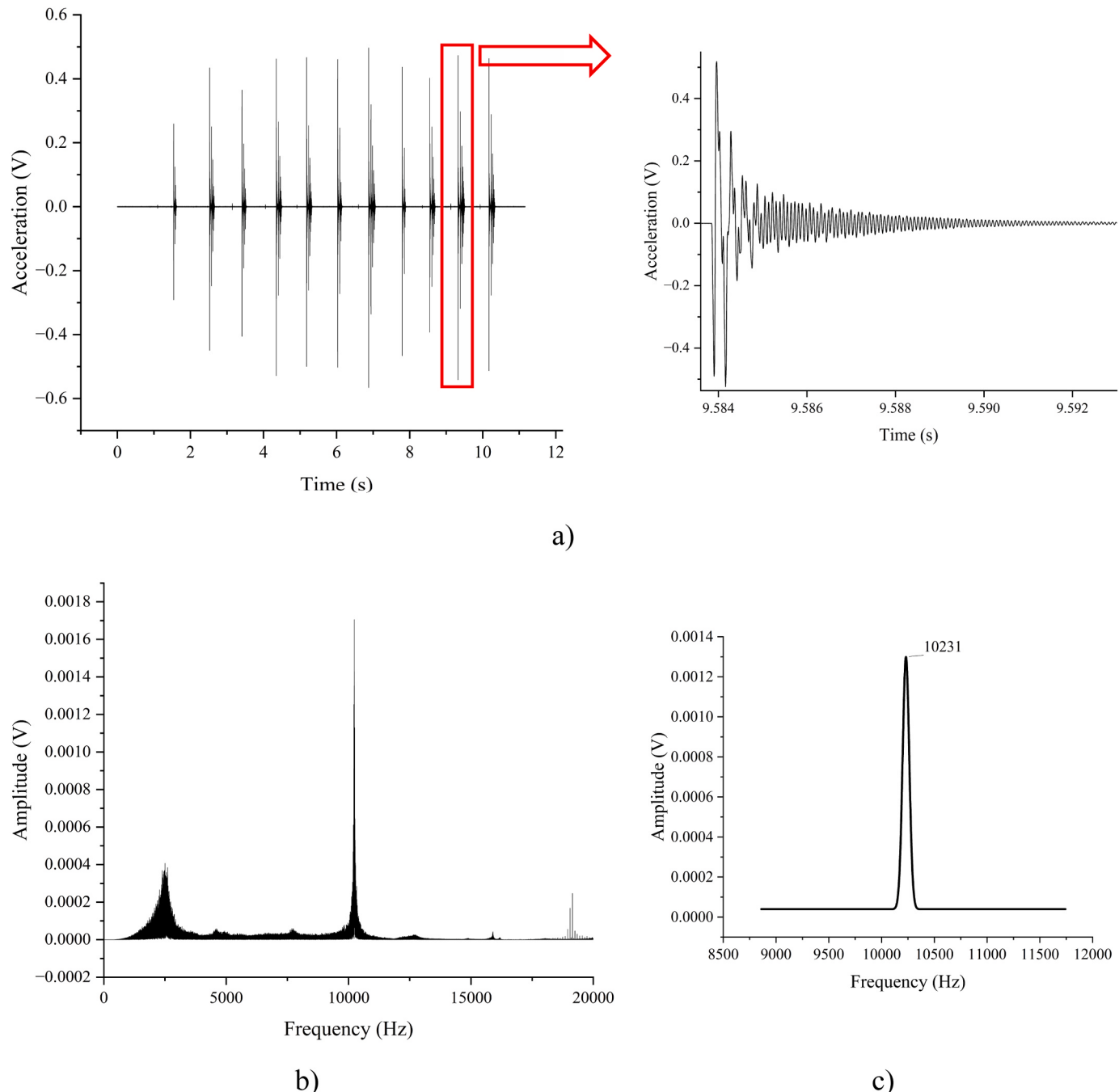


Fig. 5. Procedure for the determination of the fundamental longitudinal frequency of vibration of a prism belonging to the Ref mix: a) Free vibration response (longitudinal impact), b) Overlapped FFT spectra for a single prism, c)Fitting result of the FFT analysis of a longitudinal impact response.

The final values of the flexural strength for the mixes presented in [Table 2](#) were obtained by averaging three measurements for each set of prisms, categorized according to the temperature they were previously exposed to (room temperature, 100°C, 150°C and 200°C). Similarly, the final values of the compressive strength were calculated by averaging six measurements for each set of prisms.

3. Results and discussions

3.1. Effect of EPA

3.1.1. Mortar slump

Workability and consequently, the slump, are influenced by the

water content of the mix. A high water/cement ratio results in more workable mortar/concrete but it leads to increased chance of segregation, during casting and vibration, and a decrease in the values of mechanical properties. On the other hand, a stiff mix, results in poor compaction, leading also to a decrease in strength [\[51\]](#).

The results obtained from the mini slump cone [\[52,53\]](#) are summarized in [Table 3](#). The replacement of natural sand by EPA did not result in significant changes of the cone base diameter. The EPA10 mix showed identical behavior with the Ref mix, the same base diameter of the mini cone and the same slump, even though the water/cement ratio was increased. However, increasing the replacement percentage to 20 % and 30 % resulted in higher values of the slump even for marginal changes of the base diameter and without visible swelling of the mortar cone.

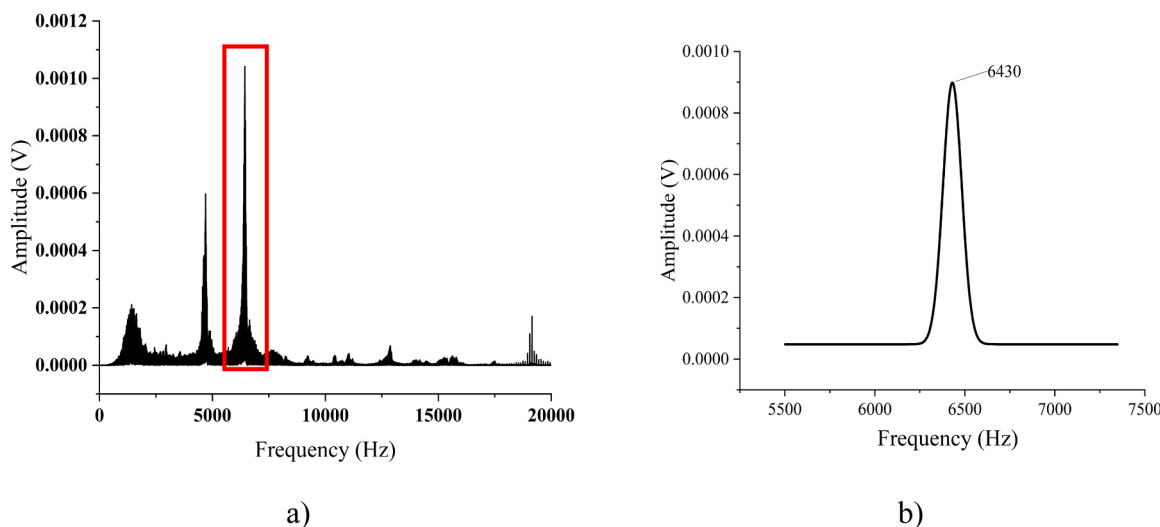


Fig. 6. Determination of the fundamental torsional frequency of vibration of a prism belonging to the Ref mix: a) Overlapped FFT spectra for a single prism, b) Fitting result of a FFT of the torsional impact response.

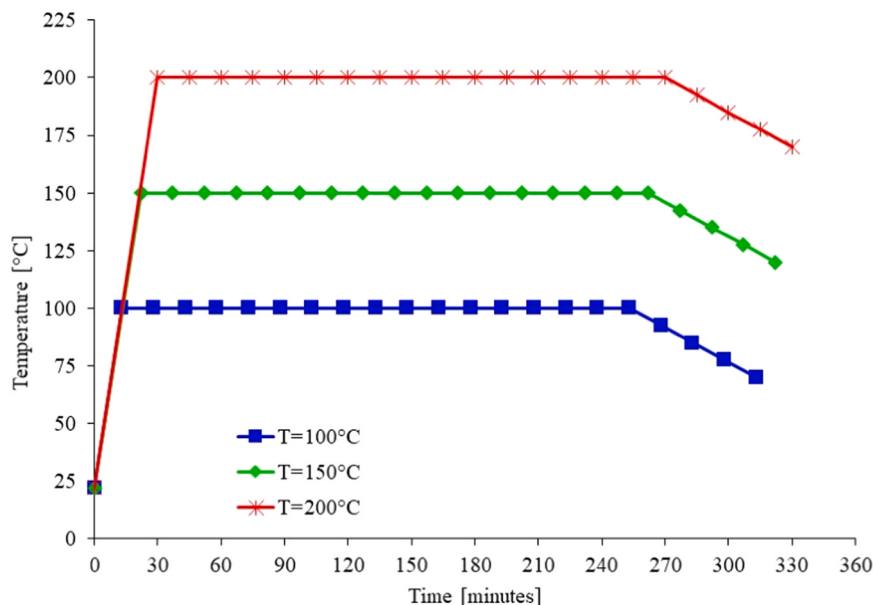


Fig. 7. Temperature-time history.

Table 3
Properties of fresh mortar.

Mix	Ref	EPA10	EPA20	EPA30
Diameter at the base [mm]	100	100	102	103
Slump [mm]	1	1	13	15

All mixes exhibited similar workability as perceived during casting the specimens. A similar approach of increasing the water/cement ratio to obtain similar workability was previously reported [54], although additives were also used, in fixed percentages for all considered mixes, to adjust the water retentivity of EPA.

3.1.2. Bulk density

The variation of density with the replacement percentage of natural sand by EPA, at the age of 28 days, is presented in Fig. 8.

A decrease in density can be observed with the increase of the replacement percentage. Compared to the reference mix, the EPA30 mix exhibited a 7.73 % reduction in density. The substitution of natural sand

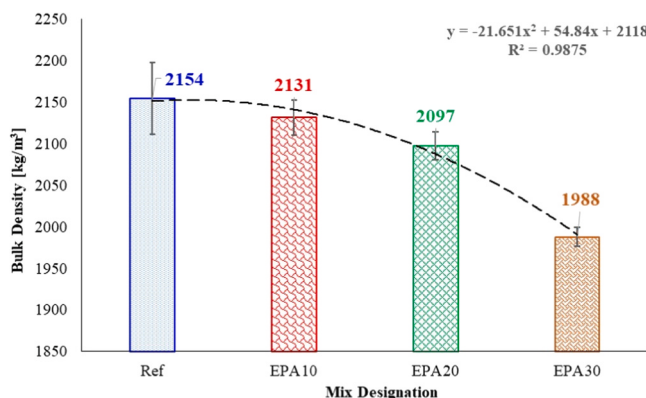


Fig. 8. Variation of density with EPA content.

with EPA led to a 1.06 % and 2.65 % decrease in density values for the EPA10 and EPA20 mixes, respectively. This downward trend appears to follow a quadratic equation, as depicted in Fig. 8.

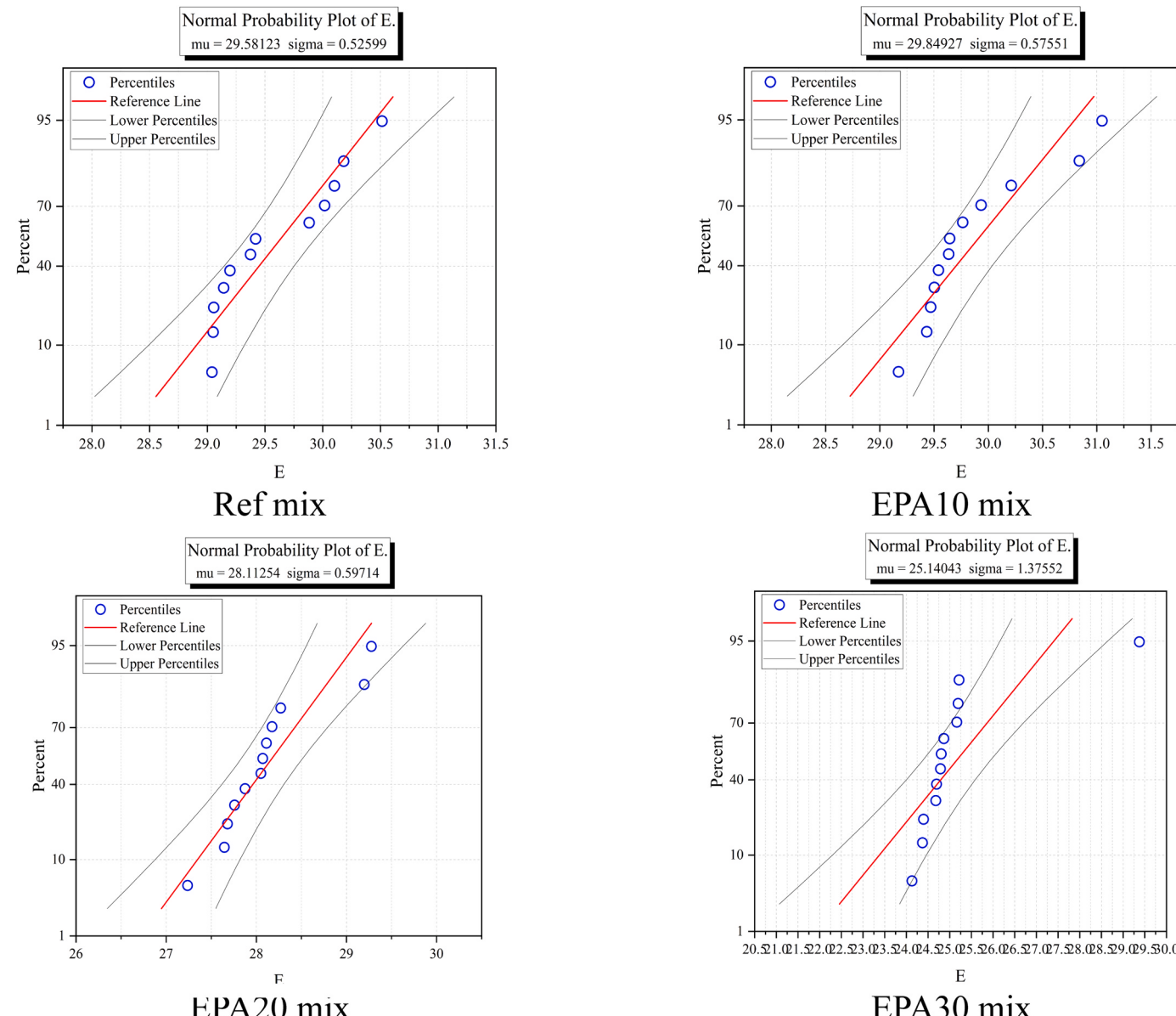


Fig. 9. Distribution of dynamic modulus of elasticity values with respect to the median.

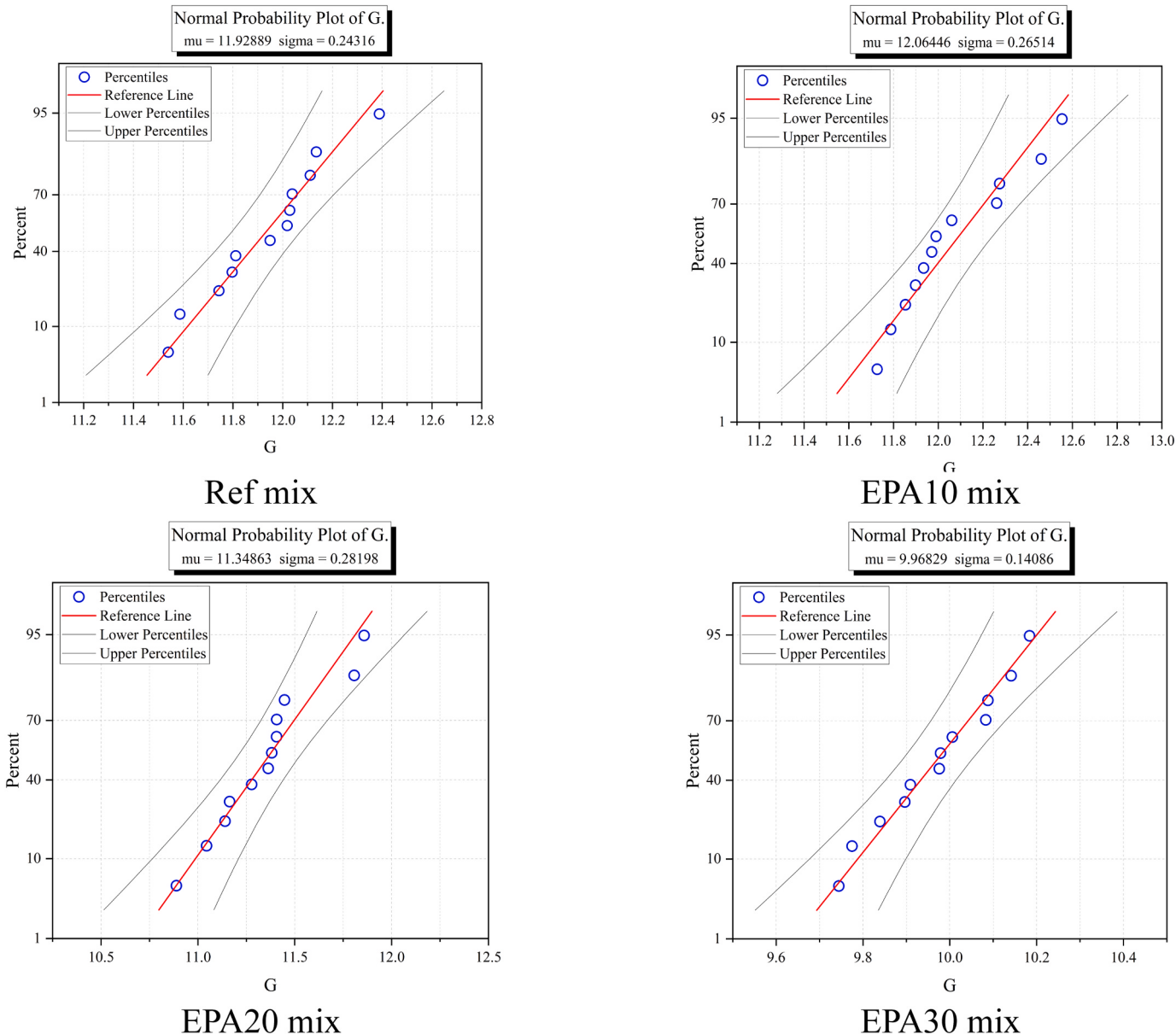


Fig. 10. Distribution of dynamic shear modulus values with respect to the median.

properties of mortar is presented in Fig. 11.

Taking into account Eqs. (1) and (2) for the calculation of the two dynamic elastic moduli, the observed trend in Fig. 11 is consistent with the data presented in Fig. 8. Since the bulk density of the mix did not change significantly, Fig. 8, and D and B coefficients from Eq. (1) and Eq. (2), respectively, are based on the geometrical dimensions of the samples, it follows that the values of the fundamental frequency of vibration for all specimens could be similar to one another. Although sand was replaced by EPA, the mass was also similar among the mixes, with small variations and showing a slight decreasing trend with increasing replacement percentage. This could be attributed to the fact that all prisms were stored in water. The data is summarized in Table 4, as average of 12 values corresponding to the 12 prisms for each mix.

The values of longitudinal (Edyn) and shear (Gdyn) dynamic moduli increased slightly when replacing 10 % of sand by EPA. For higher substitution amounts, the values for these parameters are decreasing. Nevertheless, it can be observed that the Poisson's ratio is directly proportional with the perlite quantity. This implies that Young's modulus is less affected than shear modulus, especially for over 20 %

replacement percentages, suggesting a decrease in the transversal deformability

3.1.4. Flexural tensile strength

The substitution of natural sand with EPA led to a significant reduction, ranging between 40 % and 51 %, in the flexural tensile strength values. Three prisms from each mix were tested following the procedure presented in Section 2.3.5. The results of the tests are presented in Fig. 12. Similar decreasing trends have been reported in previous research [58] although, in most cases, this was observed in specimens where perlite powder replaced Portland cement rather than sand [55,59].

3.1.5. Compressive strength

The decrease in compressive strength values was less pronounced compared to flexural strength when natural sand was replaced by EPA. The reduction ranges from 18.33 % for EPA10 to 30.71 % for EPA30, as shown in Fig. 13. Three prisms from each mix were tested, following the procedure presented in Section 2.3.5. Similar behavior regarding

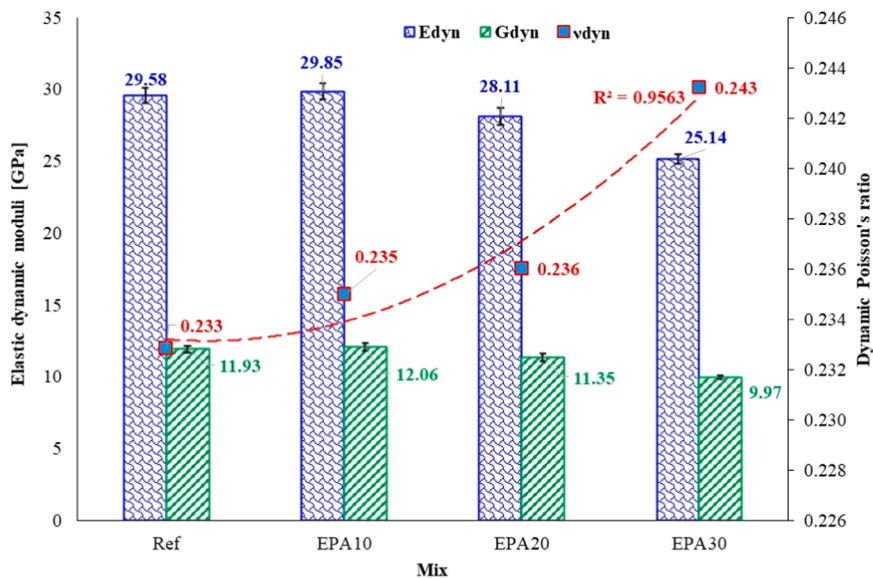


Fig. 11. Influence of EPA replacement percentage on the dynamic elastic properties of mortar.

Table 4
Dynamic characteristics of considered mixes (average values of 12 data sets).

Mix	Mass [kg]	n' (Eq. 1) [Hz]	E _{dyn} (Eq. 1) [GPa]	n'' (Eq. 2) [Hz]	G _{dyn} (Eq. 2) [GPa]	v _{dyn} (Eq. 3)
Ref	0.568	11523	29.58	6728	11.93	0.233
EPA10	0.561	11684	29.85	6829	12.06	0.235
EPA20	0.543	11440	28.11	6682	11.35	0.236
EPA30	0.532	11102	25.14	6429	9.97	0.243

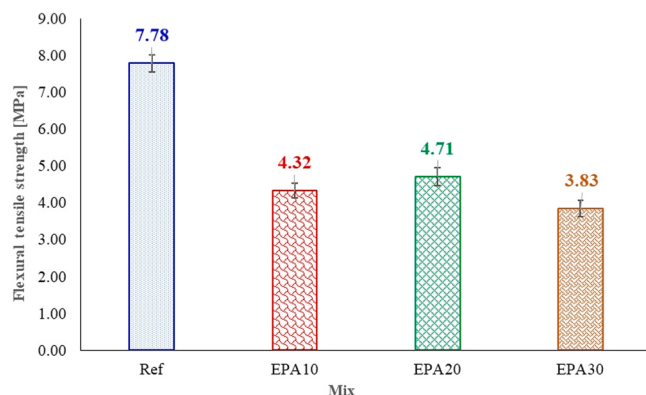


Fig. 12. Influence of EPA replacement percentage on the flexural tensile strength of mortar.

compressive strength was reported previously [58] but mostly for specimens with perlite powder replacing Portland cement instead of sand [55,59].

From the analysis of the obtained data, in terms of average values, an equation linking the dynamic longitudinal modulus of elasticity (E_{dyn}) and the compressive strength (f_c) of mortar with EPA aggregates was proposed, as shown in Eq. (4).

$$f_c = 9.08e^{-4} \cdot E_{dyn} \quad (4)$$

where both the compressive strength and the dynamic longitudinal modulus of elasticity are expressed in MPa. The accuracy of the proposed formula is checked against the experimental obtained values for the compressive strength of mortar mixes. The obtained results are

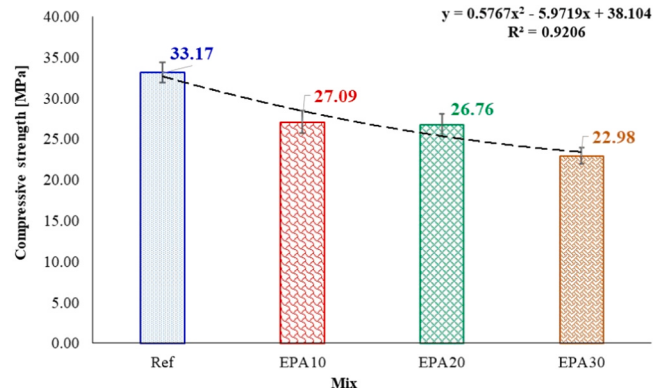


Fig. 13. Influence of EPA replacement percentage on the compressive strength of mortar.

shown in Fig. 14, in terms of average values, and in Fig. 15 in terms of individual values obtained on mortar prisms for each mix containing EPA.

From Fig. 14 it can be observed that there is a very good correlation between the values of the compressive strength given by the proposed

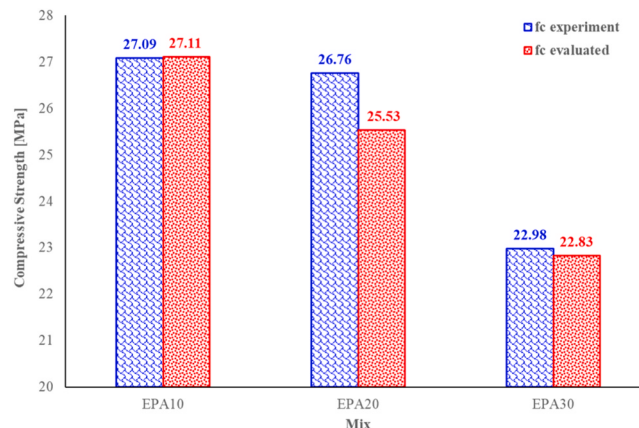


Fig. 14. Analytical vs. experimental results for the compressive strength of mortar mixes (average values).

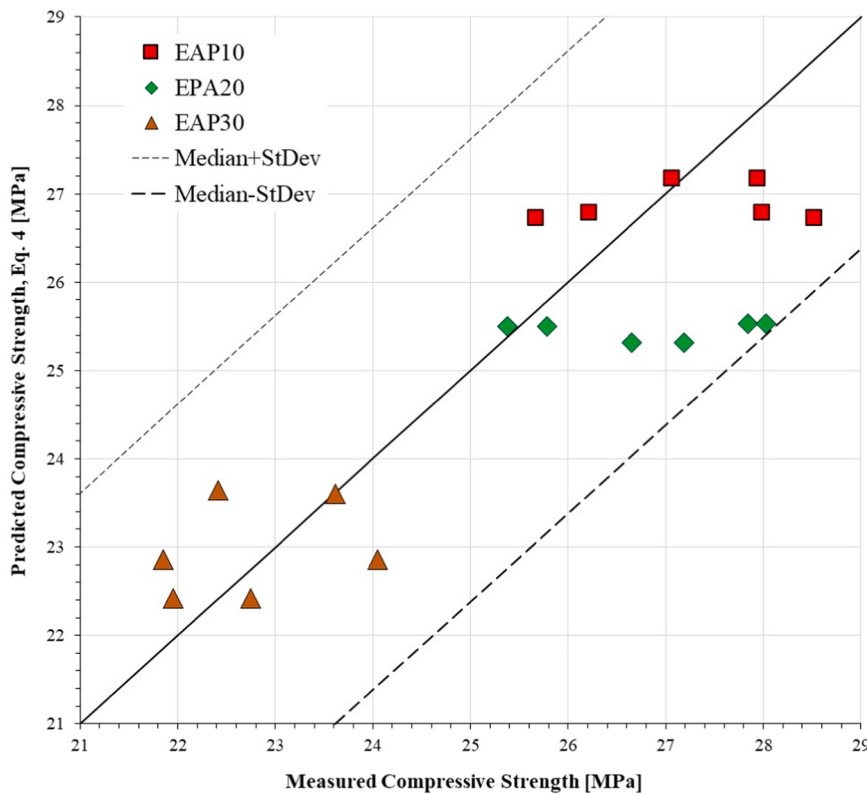


Fig. 15. Distribution of predicted/measured compressive strength values with respect to the median.

formula and the experimentally obtained data. The largest difference was obtained for EPA20 mix, 4.59 %. All other values were less than 1 % apart from the laboratory test values. The data shown in Fig. 15, obtained for individual prisms of each mix, shows that the results obtained from Eq. (4) fall within ± 1 standard deviation from the median. There is an underestimation tendency of the experimental results for 20 % and 30 % replacement rates whereas for 10 % EPA content using Eq. (4) leads to slightly overestimated results.

Surveying of the scientific literature revealed no other studies that present both dynamic elastic properties and compressive strength of mortars with EPA, thus the proposed equation could not be validated against other data sets. It is important to note that, upon further

validation, the significance of the proposed equation lies in its ability to directly and accurately determine the compressive strength of mortar with EPA once the dynamic modulus of elasticity is known. This could potentially eliminate the need for destructive tests.

The proposed equation has limitations, since it was derived for a specific cement/sand volumetric ratio, a water/cement ratio and a certain cement type. Further investigations are necessary in order to improve this equation, as reported by similar studies investigating the properties of cement-lime laying mortar [60].

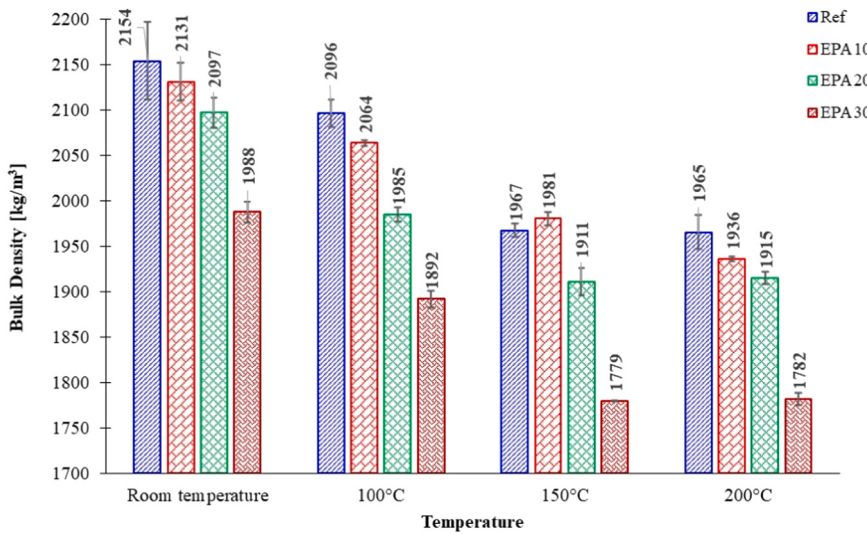


Fig. 16. Influence of temperature on the bulk density of considered mortar mixes.

3.2. Effect of temperature

As outlined in Section 2.3.4, the prismatic specimens were heated up to temperatures of 100°C, 150°C and 200°C at a rate of 6°C per minute. Subsequently, they were kept for 4 hours and then gradually cooled down back to room temperature. Specimens were analyzed in terms of density, dynamic moduli, and flexural and compressive strength.

3.2.1. Bulk density

After the thermal treatment, specimens were measured again to check for dimensional stability and weighed to account for changes in mass due to water loss. Bulk density values are presented in Fig. 16.

It can be observed that exposure to higher temperatures resulted in lower values for bulk density. Reference, EPA20 and EPA30 mixes appear to stabilize at 150°C, since exposure at 200°C does not have a notable impact on density values. EPA10 mix displays an almost linear decrease for density with the increase in temperature.

Fig. 17 illustrates the mass loss resulting from the evaporation process for each mortar mix under consideration. At 100°C, all EPA mixes exhibited a lower mass loss (4.35%–4.56%) compared to the reference (5.25%). When specimens were exposed to 150°C, both EPA20 and EPA30 mix showed a higher mass loss than Ref by 0.85% and 1.56%, respectively. The EPA10 mix registered the lowest mass loss at this temperature. At 200°C, the reference mix, EPA10 and EPA20 exhibited nearly identical mass loss values (8.77%, 9.10% and 9.20%). In contrast, EPA30 experienced the highest mass loss of 10.93%.

The variation of mass loss with temperature can be divided into two intervals: from room temperature to 150°C, and from 150°C to 200°C. In the first range of temperatures, Ref and EPA10 mixes exhibit similar trends, with a steeper slope up to 100°C, followed by a reduced rate between 100°C and 150°C. On the other hand, EPA20 and EPA30 mixes demonstrated a higher rate of mass loss from 100°C to 150°C. This phenomenon could be attributed to the increased porosity of specimens with higher percentages of EPA.

Within the temperature range of 150°C to 200°C, Ref, EPA20 and EPA30 showed little mass loss variation. This observation is supported by bulk density values depicted in Fig. 16. EPA10 exhibited an almost identical slope to the previous interval.

The observed trends can be explained by considering the internal structure of mortar. EPA are highly porous, as depicted in Fig. 3. Their use in mortar is expected to result in the formation of internal pores that are either closed or open. During heating, capillary water and water from open pores evaporates, accounting for most of the overall mass loss. It was previously reported that ettringite undergoes thermal decomposition at 90°C, while CSH begins dehydrating between 200°C and 450°C, corroborating earlier findings [47]. Additionally, excessive shrinkage of the cement paste was reported at temperatures higher than 200°C with detrimental effects in terms of strength and durability [48]. While ettringite dehydrates between 80°C and 150°C, gypsum

decomposes at 150°C–170°C and CSH starts to dehydrate at 200°C [48]. Partially saturated internal, sealed pores, resulted from water consumption during the hydration of cement grains, allow the remaining water to transform into vapors. Simultaneously, they provide enough space to prevent vapor pressure from damaging the mortar matrix. A similar phenomenon was reported in earlier research works on EPP (expanded perlite powder) used to suppress the alkali-silica reaction in cement mortar [61,62].

3.2.2. Dynamic elastic properties

Upon cooling to room temperature, the prisms were used to determine dynamic moduli, as outlined in Section 2.3.3. For each considered temperature, 3 specimens were tested, resulting in a total of 30 data sets per mix for the computation of the dynamic modulus of elasticity and the dynamic shear modulus. Results are presented in Fig. 18.

It can be observed that as the temperature increases, the values for the dynamic moduli decrease. Similar to results at room temperature, EPA10 exhibited higher dynamic elasticity modulus compared to Ref, showing improvements of 5.6%, 5.48% and 3.85% at 100°C, 150°C and 200°C, respectively. The dynamic shear modulus of EPA10 showed the highest improvement, with respect to Ref, at 150°C (6.05%). Improvements in both moduli, compared to Ref, can be seen only for EPA20 at 150°C, but they are half the ones observed for the EPA10 mix. Compared to the reference, the EPA30 mix showed consistently lower values, for both E and G, by as much as 14%.

Values for both moduli decrease almost linearly with temperature for all mixes, as it can be seen in Fig. 19. For both E and G, the temperature of 100°C represents a threshold corresponding to the most significant decrease. At this temperature, values are reduced for all mixes with percentages between 18.71% for EPA10 and 20.86% for Ref. Another important observation is that the EPA20 mix is the least affected by exposure at 150°C in comparison to 100°C.

Considering the pozzolanic nature of expanded perlite, if can be inferred that smaller pores were present in mortars with EPA [14,44]. Also, given the porous nature of EPA, modified mortars are expected to exhibit a higher total porosity compared to Ref. Nevertheless, considering bulk density values and the observed temperature effects, pore size and quantity would represent a reasonable underlying mechanism. While using 10% EPA has a beneficial effect on elastic properties, higher percentages prove detrimental, possibly due to the availability of calcium hydroxide (CH) in the cementitious matrix [63].

3.2.3. Flexural tensile strength

The impact of temperature exposure on the flexural tensile strength of all mortar mixes is shown in Fig. 20. It can be observed that all EPA mixes exhibit lower values than Ref, at both room temperature and 100°C. Conversely, at higher temperatures all EPA mortars show higher tensile strengths, compared to both the reference mix and to lower treatment temperature values.

At the same time, it can be seen that while the flexural tensile strength of the Ref mix exhibits a decreasing trend with the increase in temperature, EPA mixes showed an opposite behavior. All recorded values of the flexural tensile strength at 100°C, 150°C and 200°C were higher than the value obtained at room temperature. EPA10 and EPA20 mixes registered a peak increase at 150°C while the value for the EPA30 mix continuously increased with the increase in the exposure temperature, although only a 3.5% increase was observed from 150°C to 200°C.

Tensile strength values of EPA mortars at all temperatures, normalized to the Ref value at each temperature, are presented in Fig. 21. The EPA10 can be seen to exhibit a steeper increase compared to the other two mixes. Comparing Fig. 20 and Fig. 21, it can be inferred that EPA20 and EPA30 display similar trends in both absolute and normalized values. On the other hand, normalized values of EPA10 are seen to continuously increase, suggesting that flexural strength is more affected for Ref than for EPA10, when increasing the temperature from 150°C to 200°C.

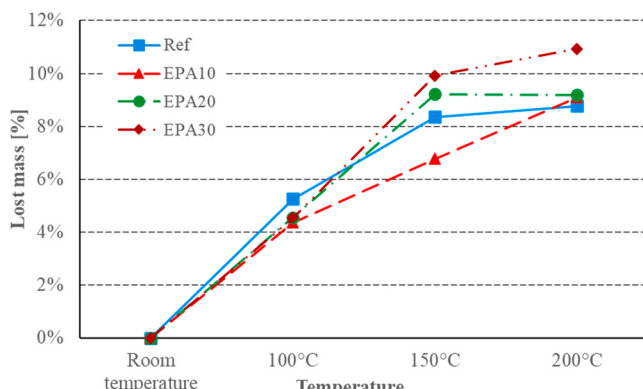


Fig. 17. Lost mass of mortar prisms as function of temperature.

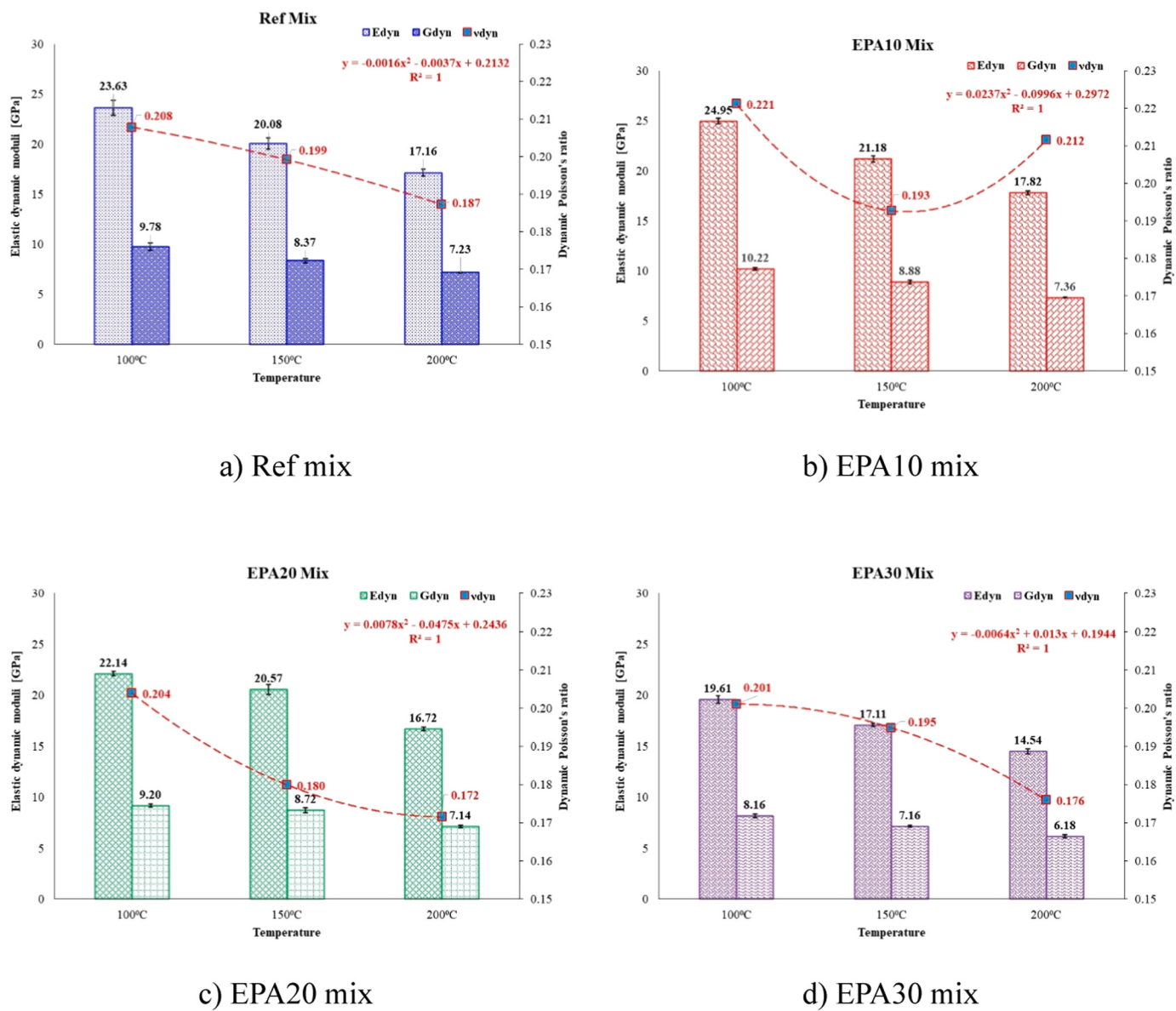


Fig. 18. Temperature influence on the dynamic elastic properties of mortars.

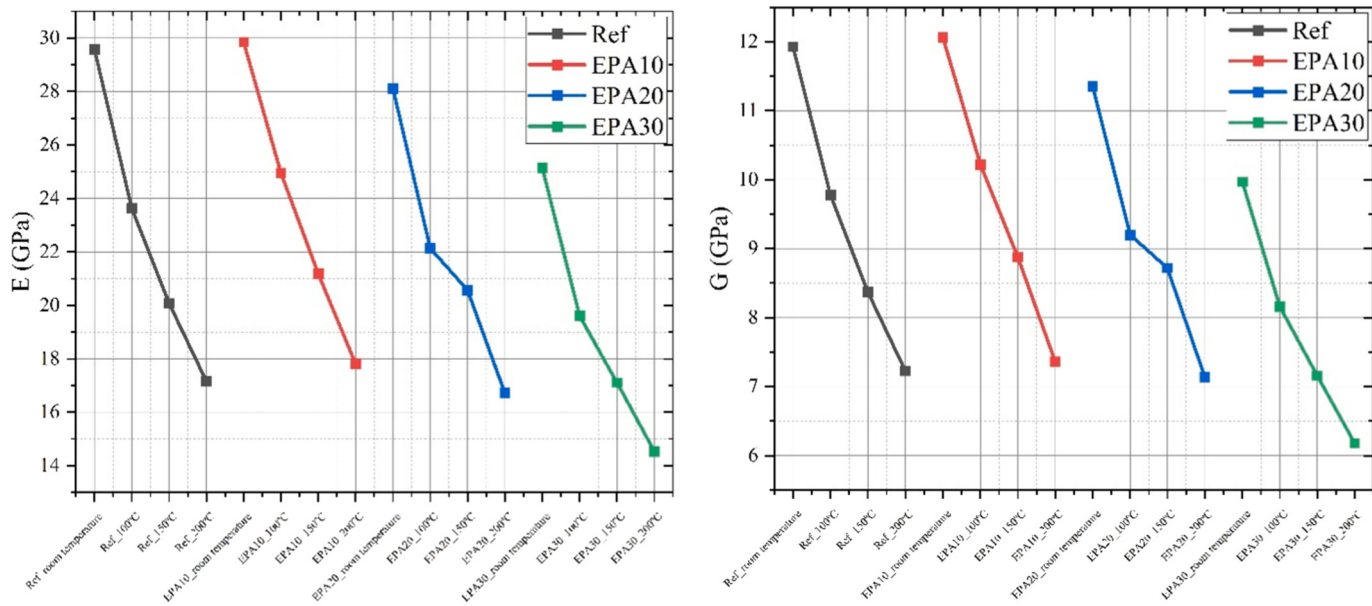
A possible explanation of the obtained results may reside in the pozzolanic nature of expanded perlite aggregates. Recent studies confirmed that, due to pozzolanic activity, the larger pores in the cement matrix are transformed into smaller pores because of the hydration products [44,64,65]. At the same time, no deteriorations in the cementitious matrix were reported for temperatures up to 400°C [44]. However, pozzolanic reaction needs time and requires a higher activation energy than the case of using Portland cement alone. This accounts for the lower early age mechanical properties in cement-based materials with various pozzolans. One method to accelerate the rate of pozzolanic activity is to increase the curing temperature. However, this approach was reported to influence the degree of crystallinity of the resulting CSH [63]. On the other hand, when subjecting cement-based mortar to elevated temperature, lower mass losses were reported for mixes with calcined perlite [66]. This implies that the presence of expanded perlite positively influences the behavior of mortar at elevated temperatures.

3.2.4. Compressive strength

The effect of exposure temperature on compressive strength for all mortar mixes is presented in Fig. 22. An increase in temperature resulted

in decreasing values of the Ref compressive strength, with a steep decrease of 19.35 % at 100°C, and additional reductions of 4 % for 150°C and 200°C. The compressive strength values of EPA10 and EPA20 mixes decreased when exposed to 100°C. However, at 150°C and 200°C, both mixes showed higher values compared to both the Ref mix at the same temperature and to their room temperature values. This suggests that a lower content of EPA led to an improved internal structure, potentially related to lower porosity. Additionally, subjecting the EPA specimens to higher temperatures and subsequent cooling to room temperature may have promoted an acceleration of the pozzolanic reaction [44,63–66] and the rehydration of cement grains [49].

The substitution of natural sand by EPA resulted in higher normalized values of the compressive strength with respect to the Ref mix, Fig. 23, compared to the flexural strength, Fig. 21. At the same time, the compressive strength gains when subjected to elevated temperature are lower than in the case of flexural strength for all EPA mixes. This may be attributed to a different CSH crystallinity, due to the promotion of pozzolanic reaction at elevated temperatures, that had a more significant influence on the values of the compressive strength. Similar trends as the ones shown in Figs. 21 and 23 were previously reported [67],



a) Dynamic longitudinal modulus of elasticity

b) Dynamic shear modulus

Fig. 19. Decreasing trends of the two dynamic moduli as function of temperature.

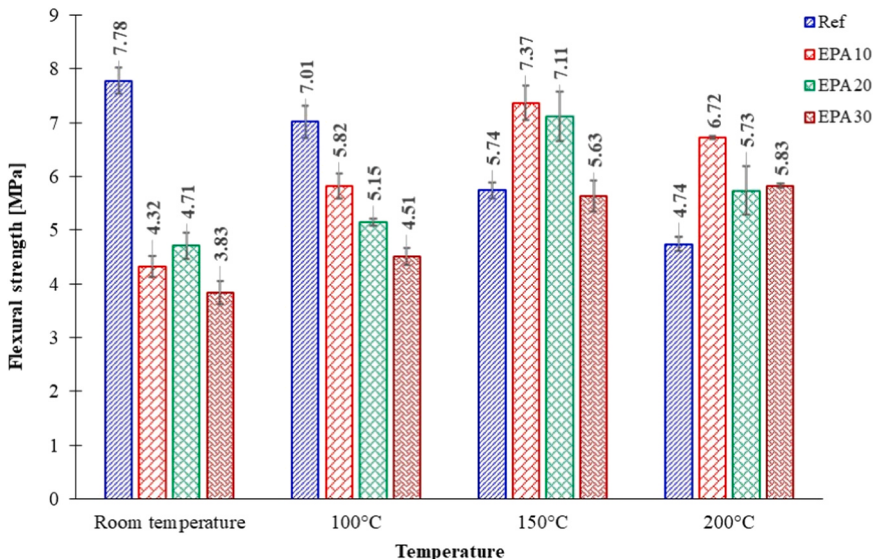


Fig. 20. Influence of temperature on the flexural tensile strength values.

although for higher temperatures and higher replacement percentages [68].

4. Conclusions

The present paper aims at bringing its contribution to narrowing the knowledge gap on the use of EPA in cement-based mortar, both at room and at temperatures up to 200°C. Previous studies reported improvements in the mechanical properties of concrete containing powder perlite for temperatures up to 300°C. Therefore, the parameters considered in this research were: the replacement percentage (10 %, 20 % and 30 % by volume) of natural sand by EPA with a maximum grain size of 4 mm and the temperature treatment of mortar prisms at the age of 28 days. The selected temperatures were 100°C, 150°C and 200°C. The influence of both parameters on the flexural and

compressive strength of mortar as well as dynamic elastic properties were experimentally determined. Based on the results presented in the paper, the following conclusions can be drawn:

1. Substituting sand by expanded perlite aggregates, by volume, results in a decrease in the values of density, flexural strength and compressive strength at the age of 28 days. The higher the substitution percentage, the higher the decrease.
2. When substitution percentage of sand by EPA is 10 % or 20 %, very little influence is observed from the point of view of dynamic longitudinal modulus of elasticity and shear modulus of prismatic specimens.
3. An empirical equation is proposed to obtain the compressive strength of mortar with EPA aggregates when the dynamic longitudinal modulus of elasticity (E_{dyn}) is known. The proposed equation shows

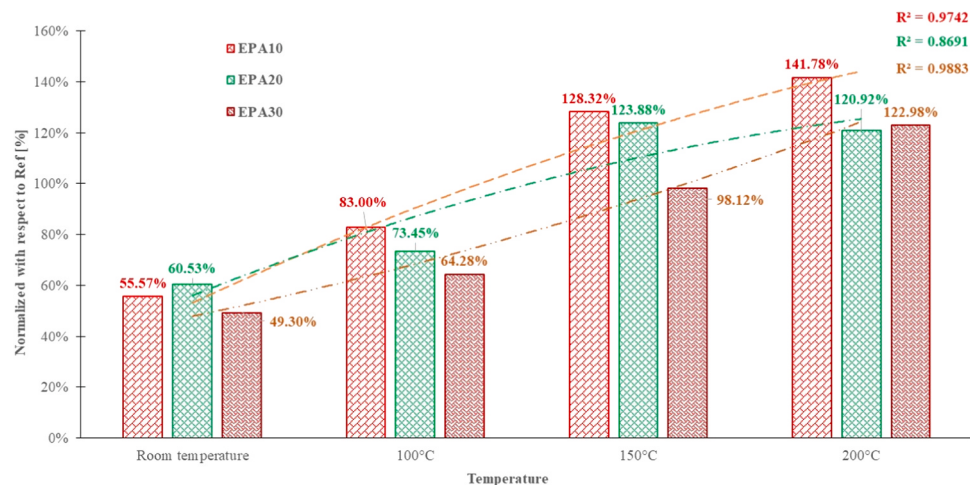


Fig. 21. Flexural tensile strength of EPA mixes normalized with respect to the Ref mix.

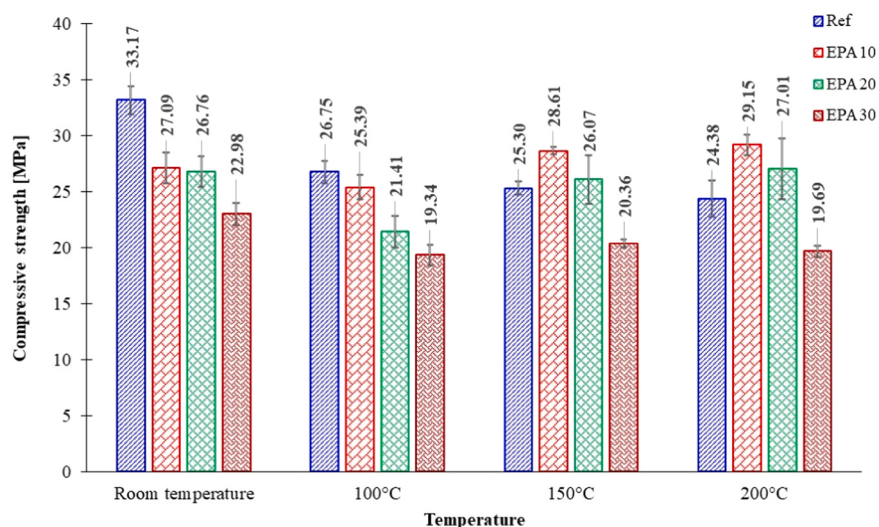


Fig. 22. Influence of temperature on the compressive strength values.

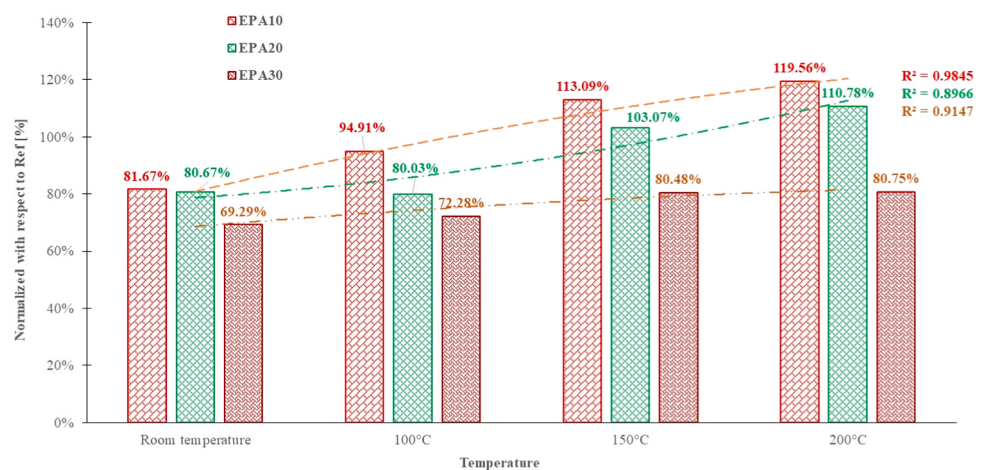


Fig. 23. Compressive strength of EPA mixes normalized with respect to the Ref mix.

- good accuracy of the predicted values when compared to experimental data. While further validation is necessary, the scientific literature currently lacks reports on these parameters for cement mortar with EPA.
4. Exposing the specimens to temperatures of 100°C, 150°C and 200°C results in a decrease in the values of bulk density due, mostly, to the evaporation process of capillary water. Expanded perlite mortar mixes exhibit a more pronounced density reduction due to the porous nature of these aggregates.
 5. Similar decreasing trends are reported for the values of dynamic moduli of all considered mortar mixes. However, for EPA10 and EPA20 mixes, higher values are reported compared to the Ref mix, without expanded perlite aggregates. This can be attributed to smaller internal pores dimensions. However, further research is necessary to confirm this hypothesis by either computed tomography (CT) or mercury intrusion porosimetry (MIP).
 6. While the flexural tensile strength of Ref mix decreased with the increase in temperature, all EPA mixes show higher values after being subjected to selected temperatures compared to the one obtained at room temperature. The highest values are obtained for the EPA10 and EPA20 mixes at 150°C. The obtained values are also higher than the one obtained for the Ref mix at the considered temperature
 7. A similar conclusion can be drawn from the point of view of the compressive strength of mortar mixes. The highest values are obtained for EPA10 and EPA20 mixes at 200°C, although the increase is only marginal. At both 150°C and 200°C the compressive strength of EPA10 and EPA20 mixes are higher than the Ref mix.
 8. When taking into account both the temperature and the replacement percentage of natural sand by EPA, the optimum combinations are obtained for 10 % and 20 % replacement percentages at temperatures between 100°C and 150°C for the dynamic moduli of elasticity. The same replacement percentages result in improved flexural and compressive strength values at 150°C. Higher replacement percentages, e.g. 30 % as considered in this research, results in consistently lower values for the investigated parameters, with the exception of flexural strength, at both room and temperatures up to 200°C.

CRediT authorship contribution statement

Ana-Maria Toma: Writing – original draft, Validation, Methodology, Conceptualization. **Ioana Olteanu:** Writing – original draft, Methodology, Investigation, Formal analysis. **George Tararu:** Writing – review & editing, Methodology, Investigation, Formal analysis. **Ionut-Ovidiu Toma:** Writing – original draft, Supervision, Resources, Project administration, Methodology, Investigation, Funding acquisition, Formal analysis, Data curation, Conceptualization. **Cristian Pastia:** Writing – review & editing, Methodology, Investigation, Formal analysis. **Georgiana Bunea:** Writing – review & editing, Visualization, Methodology, Investigation, Formal analysis. **Sergiu-Mihai Alexa-Stratulat:** Writing – original draft, Validation, Supervision, Software, Methodology, Investigation, Formal analysis, Data curation.

Declaration of Competing Interest

The authors declare that they have no known competing financial interests or personal relationships that could have appeared to influence the work reported in this paper.

Data availability

Data will be made available on request.

Acknowledgment

The research presented in this paper was conducted as part of the PN-

III-P2-2.1-PED-2021-0677 research grant “Sustainable Concrete for Energy Efficient Buildings” funded by Executive Agency for Higher Education, Research, Development and Innovation Funding – UEFISCDI.

References

- [1] GCCAssociation, Cement and Concrete Around the World, Glob. Cem. Concr. Assoc. (2020). <https://gccassociation.org/concretefuture/cement-concrete-around-the-world/>.
- [2] P.M. Borges, J.Z. Schiavon, S.R. da Silva, E. Rigo, A. Neves Junior, E. Possan, J.J. de O. Andrade, Mortars with recycled aggregate of construction and demolition waste: mechanical properties and carbon uptake, Constr. Build. Mater. 387 (2023) 131600, <https://doi.org/10.1016/j.conbuildmat.2023.131600>.
- [3] H. Shoukry, P. Perumal, A. Abadel, H. Alghamdi, M. Alamri, H.A. Abdel-Gawad, Performance of limestone-calcined clay cement mortar incorporating high volume ferrochrome waste slag aggregate, Constr. Build. Mater. 350 (2022) 128928, <https://doi.org/10.1016/j.conbuildmat.2022.128928>.
- [4] P. Matar, J. Barhoun, Effects of waterproofing admixture on the compressive strength and permeability of recycled aggregate concrete, J. Build. Eng. 32 (2020) 101521, <https://doi.org/10.1016/j.jobe.2020.101521>.
- [5] U. Chandru, B. A, S. R, Systematic comparison of different recycled fine aggregates from construction and demolition wastes in OPC concrete and PPC concrete, J. Build. Eng. (2023) 106768, <https://doi.org/10.1016/j.jobe.2023.106768>.
- [6] M.J. Ashraf, M. Idrees, A. Akbar, Performance of silica fume slurry treated recycled aggregate concrete reinforced with carbon fibers, J. Build. Eng. 66 (2023) 105892, <https://doi.org/10.1016/j.jobe.2023.105892>.
- [7] F. Rezaei, A. Memarzadeh, M.-R. Davoodi, M.-A. Dashab, M. Nematzadeh, Mechanical features and durability of concrete incorporating recycled coarse aggregate and nano-silica: experimental study, prediction, and optimization, J. Build. Eng. 73 (2023) 106715, <https://doi.org/10.1016/j.jobe.2023.106715>.
- [8] L. Barbieri, F. Altimari, F. Andreola, B. Maggi, I. Lancellotti, Characterization of volcano-sedimentary rocks and related scraps for design of sustainable materials, Materials 16 (2023) 3408, <https://doi.org/10.3390/ma16093408>.
- [9] W.H. Juimo Tchamdjou, T. Cherradi, M.L. Abidi, L.A. Pereira-de-Oliveira, Mechanical properties of lightweight aggregates concrete made with cameronian volcanic scoria: destructive and non-destructive characterization, J. Build. Eng. 16 (2018) 134–145, <https://doi.org/10.1016/j.jobe.2018.01.003>.
- [10] M. Pekgöz, İ. Tekin, Microstructural investigation and strength properties of structural lightweight concrete produced with Zeolitic tuff aggregate, J. Build. Eng. 43 (2021) 102863, <https://doi.org/10.1016/j.jobe.2021.102863>.
- [11] A.M. Rashad, A synopsis about perlite as building material – a best practice guide for Civil Engineer, Constr. Build. Mater. 121 (2016) 338–353, <https://doi.org/10.1016/j.conbuildmat.2016.06.001>.
- [12] S. Celik, R. Family, M.P. Menguc, Analysis of perlite and pumice based building insulation materials, J. Build. Eng. 6 (2016) 105–111, <https://doi.org/10.1016/j.jobe.2016.02.015>.
- [13] M. Davraz, M. Koru, A.E. Akdag, Kilincarslan, Y.E. Delikanli, M. Çabuk, Investigating the use of raw perlite to produce monolithic thermal insulation material, Constr. Build. Mater. 263 (2020) 120674, <https://doi.org/10.1016/j.conbuildmat.2020.120674>.
- [14] E. Kapeluszna, Ł. Kotwica, W. Nocuń-Wczelik, Comparison of the effect of ground waste expanded perlite and silica fume on the hydration of cements with various tricalcium aluminate content – comprehensive analysis, Constr. Build. Mater. 303 (2021) 124434, <https://doi.org/10.1016/j.conbuildmat.2021.124434>.
- [15] United States Geological Survey (USGS), Mineral commodity summaries 2023, 2023. doi:10.31133/mcs2023.
- [16] M. Zukowski, G. Haese, Experimental and numerical investigation of a hollow brick filled with perlite insulation, Energy Build. (2010), <https://doi.org/10.1016/j.enbuild.2010.03.009>.
- [17] M. Výšvaril, M. Pavlíková, M. Záleská, A. Pivák, T. Žižlavský, P. Rovnaníková, P. Bayer, Z. Pavlik, Non-hydrophobized perlite renders for repair and thermal insulation purposes: influence of different binders on their properties and durability, Constr. Build. Mater. 263 (2020) 120617, <https://doi.org/10.1016/j.conbuildmat.2020.120617>.
- [18] Y. Fang, X. Yin, P. Cui, X. Wang, K. Zhuang, Z. Ding, F. Xing, Properties of magnesium potassium phosphate cement-expanded perlite composites applied as fire resistance coating, Constr. Build. Mater. 293 (2021) 123513, <https://doi.org/10.1016/j.conbuildmat.2021.123513>.
- [19] S.M. Motahari Karein, P. Vosoughi, S. Isapour, M. Karakouzian, Pretreatment of natural perlite powder by further milling to use as a supplementary cementitious material, Constr. Build. Mater. (2018), <https://doi.org/10.1016/j.conbuildmat.2018.08.012>.
- [20] H. Li, L. Wang, Y. Zhang, J. Yang, D.C.W. Tsang, V. Mechtcherine, Biochar for sustainable construction industry, in: Curr. Dev. Biotechnol. Bioeng., Elsevier, 2023, pp. 63–95, <https://doi.org/10.1016/B978-0-323-91873-2.00015-7>.
- [21] Ł. Kotwica, W. Pichór, E. Kapeluszna, A. Różycka, Utilization of waste expanded perlite as new effective supplementary cementitious material, J. Clean. Prod. 140 (2017) 1344–1352, <https://doi.org/10.1016/j.jclepro.2016.10.018>.
- [22] S.M.M. Karein, A. Joshaghani, A.A. Ramezaniyanpour, S. Isapour, M. Karakouzian, Effects of the mechanical milling method on transport properties of self-compacting concrete containing perlite powder as a supplementary cementitious material, Constr. Build. Mater. 172 (2018) 677–684, <https://doi.org/10.1016/j.conbuildmat.2018.03.205>.

- [23] S. Alexander, S. Juhi Manohar, S. Shino John, K. Varun Teja, T. Meena, Mechanical and micro-structural properties of perlite powder incorporated SCC, *Mater. Today Proc.* 45 (2021) 3374–3382, <https://doi.org/10.1016/j.matpr.2020.12.776>.
- [24] D. Fodil, M. Mohamed, Compressive strength and corrosion evaluation of concretes containing pozzolana and perlite immersed in aggressive environments, *Constr. Build. Mater.* 179 (2018) 25–34, <https://doi.org/10.1016/j.conbuildmat.2018.05.190>.
- [25] X. Wang, D. Wu, Q. Geng, D. Hou, M. Wang, L. Li, P. Wang, D. Chen, Z. Sun, Characterization of sustainable ultra-high performance concrete (UHPC) including expanded perlite, *Constr. Build. Mater.* 303 (2021) 124245, <https://doi.org/10.1016/j.CONBUILDMAT.2021.124245>.
- [26] M. Bakhti, A. Dalalbashi, H. Soheili, Energy dissipation capacity of an optimized structural lightweight perlite concrete, *Constr. Build. Mater.* 389 (2023) 131765, <https://doi.org/10.1016/j.conbuildmat.2023.131765>.
- [27] R. Demirboğa, I. Örting, R. Güll, Effects of expanded perlite aggregate and mineral admixtures on the compressive strength of low-density concretes, *Cem. Concr. Res.* (2001), [https://doi.org/10.1016/S0008-8846\(01\)00615-9](https://doi.org/10.1016/S0008-8846(01)00615-9).
- [28] M. Abed, J. de Brito, Evaluation of high-performance self-compacting concrete using alternative materials and exposed to elevated temperatures by non-destructive testing, *J. Build. Eng.* 32 (2020) 101720, <https://doi.org/10.1016/j.jobe.2020.101720>.
- [29] ASRO (Romanian Standards Association), SR EN 197-1: Cement. Part I: Composition, specifications and conformity criteria for normal use cements, (2011).
- [30] A. Favier, C. De Wolf, K. Scrivener, G. Habert, A Sustainable Future for the European Cement and Concrete Industry, Zurich, 2018. (https://europeancimate.org/wp-content/uploads/2018/10/AB_SP_Decarbonisation_report.pdf).
- [31] ASRO (Romanian Standards Association), SR EN 1097-2:2002 Tests for mechanical and physical properties of aggregates - Part 2: Methods for the determination of resistance to fragmentation, (2020). (<https://magazin.asro.ro/ro/standard/274070>).
- [32] ASRO (Romanian Standards Association), SR EN 933-2:2020 Tests for geometrical properties of aggregates. Determination of particle size distribution. Test sieves, nominal size of apertures, (2020). (<https://magazin.asro.ro/ro/standard/274810>).
- [33] S. Grzeszczyk, G. Janus, Lightweight reactive powder concrete containing expanded perlite, *Materials* 14 (2021) 3341, <https://doi.org/10.3390/ma14123341>.
- [34] ASTM International, ASTM C618-22: Standard Specification for Coal Fly Ash and Raw or Calcined Natural Pozzolan for Use in Concrete, (2022). doi:[10.1520/C0618-22](https://doi.org/10.1520/C0618-22).
- [35] ASTM International, ASTM C 618: Standard Specification for Coal Fly Ash and Raw or Calcined Natural Pozzolan for Use in Concrete, (2022). (<https://www.astm.org/c0618-22.html>).
- [36] D. Adi Darmawan, A. Wahyudi, H. Eric Mamby, I. Suherman, Characterization of perlite and expanded perlite from West Sumatra, Indonesia, *IOP Conf. Ser. Earth Environ. Sci.* 882 (2021) 012010, <https://doi.org/10.1088/1755-1315/882/1/012010>.
- [37] M. Lanzón, F.J. Castellón, M. Ayala, Effect of the expanded perlite dose on the fire performance of gypsum plasters, *Constr. Build. Mater.* 346 (2022) 128494, <https://doi.org/10.1016/j.conbuildmat.2022.128494>.
- [38] H. AzariJafari, A. Kazemian, B. Ahmadi, J. Berenjian, M. Shekarchi, Studying effects of chemical admixtures on the workability retention of zeolitic Portland cement mortar, *Constr. Build. Mater.* 72 (2014) 262–269, <https://doi.org/10.1016/j.conbuildmat.2014.09.020>.
- [39] ASRO (Romanian Standards Association), SR EN 196-1:2016, Methods of testing cement - Part 1: Determination of Strength, (2016).
- [40] H. Dilbas, Effect of cement type and water-to-cement ratio on fresh properties of superabsorbent polymer-modified cement paste, *Materials* 16 (2023) 2614, <https://doi.org/10.3390/ma16072614>.
- [41] I.-O. Toma, G. Stoian, M.-M. Rusu, I. Ardelean, N. Cimpoeșu, S.-M. Alexa-Stratulat, Analysis of pore structure in cement pastes with micronized natural zeolite, *Materials* 16 (2023) 4500, <https://doi.org/10.3390/ma16134500>.
- [42] ASTM International, ASTM C215-19 - Standard Test Method for Fundamental Transverse, Longitudinal, and Torsional Resonant Frequencies of Concrete Specimens, (2019).
- [43] D.P. Thanaraj, A.N., P. Arulraj, K. Al-Jabri, Investigation on structural and thermal performance of reinforced concrete beams exposed to standard fire, *J. Build. Eng.* 32 (2020) 101764, <https://doi.org/10.1016/j.jobe.2020.101764>.
- [44] M. Saridemir, A. Yıldırım, Effect of elevated temperatures on properties of high strength mortars containing ground calcined diatomite with limestone sand, *J. Build. Eng.* 56 (2022) 104748, <https://doi.org/10.1016/j.jobe.2022.104748>.
- [45] S. Alani, M.S. Hassan, A.A. Jaber, I.M. Ali, Effects of elevated temperatures on strength and microstructure of mortar containing nano-calcined montmorillonite clay, *Constr. Build. Mater.* 263 (2020) 120895, <https://doi.org/10.1016/j.conbuildmat.2020.120895>.
- [46] I. Fletcher, S. Welch, J. Torero, R. Carvel, A. Usmani, Behaviour of concrete structures in fire, *Therm. Sci.* 11 (2007) 37–52, <https://doi.org/10.2298/TSCI0702037F>.
- [47] J. Piasta, Heat deformations of cement paste phases and the microstructure of cement paste, *Mater. Struct.* 17 (1984) 415–420, <https://doi.org/10.1007/BF02473981>.
- [48] I. Hager, Behaviour of cement concrete at high temperature, *Bull. Pol. Acad. Sci. Tech. Sci.* 61 (2013) 145–154, <https://doi.org/10.2478/bpasts-2013-0013>.
- [49] P. Sikora, K. Cendrowski, E. Horszczaruk, E. Mijowska, The effects of Fe₃O₄ and Fe₃O₄/SiO₂ nanoparticles on the mechanical properties of cement mortars exposed to elevated temperatures, *Constr. Build. Mater.* 182 (2018) 441–450, <https://doi.org/10.1016/j.conbuildmat.2018.06.133>.
- [50] M. Castellote, C. Alonso, C. Andrade, X. Turrillas, J. Campo, Composition and microstructural changes of cement pastes upon heating, as studied by neutron diffraction, *Cem. Concr. Res.* 34 (2004) 1633–1644, [https://doi.org/10.1016/S0008-8846\(03\)00229-1](https://doi.org/10.1016/S0008-8846(03)00229-1).
- [51] M. Vijayalakshmi, A.S.S. Sekar, G. Ganesh prabhu, Strength and durability properties of concrete made with granite industry waste, *Constr. Build. Mater.* 46 (2013) 1–7, <https://doi.org/10.1016/j.conbuildmat.2013.04.018>.
- [52] F. Šoukal, L. Bocian, R. Novotný, L. Dlabajová, N. Šuleková, J. Hajzler, O. Koutný, M. Drdlová, The effects of silica fume and superplasticizer type on the properties and microstructure of reactive powder concrete, *Materials* 16 (2023) 6670, <https://doi.org/10.3390/ma162006670>.
- [53] H. Varela, G. Barluenga, I. Palomar, A. Sepulcre, Synergies on rheology and structural build-up of fresh cement pastes with nanoclays, nanosilica and viscosity modifying admixtures, *Constr. Build. Mater.* 308 (2021) 125097, <https://doi.org/10.1016/j.conbuildmat.2021.125097>.
- [54] M. Lanzón, P.A. García-Ruiz, Lightweight cement mortars: advantages and inconveniences of expanded perlite and its influence on fresh and hardened state and durability, *Constr. Build. Mater.* 22 (2008) 1798–1806, <https://doi.org/10.1016/j.CONBUILDMAT.2007.05.006>.
- [55] F. Guenanou, H. Khelafi, A. Attache, Behavior of perlite-based mortars on physicochemical characteristics, mechanical and carbonation: case of perlite of Hammam Bougrara, *J. Build. Eng.* 24 (2019) 100734, <https://doi.org/10.1016/j.jobe.2019.100734>.
- [56] D. Kramar, V. Bindiganavile, Impact response of lightweight mortars containing expanded perlite, *Cem. Concr. Compos.* 37 (2013) 205–214, <https://doi.org/10.1016/j.cemconcomp.2012.10.004>.
- [57] A. Łagisz, D. Olszowski, W. Pichór, L. Kotwica, Quantitative determination of processed waste expanded perlite performance as a supplementary cementitious material in low emission blended cement composites, *J. Build. Eng.* 40 (2021) 102335, <https://doi.org/10.1016/j.jobe.2021.102335>.
- [58] V. Akyüncü, F. Sanlıturk, Investigation of physical and mechanical properties of mortars produced by polymer coated perlite aggregate, *J. Build. Eng.* 38 (2021) 102182, <https://doi.org/10.1016/j.jobe.2021.102182>.
- [59] K. Şengül, S.T. Erdogan, Influence of ground perlite on the hydration and strength development of calcium aluminate cement mortars, *Constr. Build. Mater.* 266 (2021) 120943, <https://doi.org/10.1016/j.conbuildmat.2020.120943>.
- [60] G.H. Nalon, M.A. Alves, L.G. Pedrotti, J.C. Lopes Ribeiro, W.E. Hilarino Fernandes, D. Silva da Oliveira, Compressive strength, dynamic, and static modulus of cement-lime laying mortars obtained from samples of various geometries, *J. Build. Eng.* 44 (2021) 102626, <https://doi.org/10.1016/j.jobe.2021.102626>.
- [61] F. Bektaş, L. Turanlı, P.J.M. Monteiro, Use of perlite powder to suppress the alkali-silica reaction, *Cem. Concr. Res.* 35 (2005) 2014–2017, <https://doi.org/10.1016/j.cenconres.2004.10.029>.
- [62] R. Chihaioui, H. Siad, Y. Senhadji, M. Mouli, A.M. Nefoussi, M. Lachemi, Efficiency of natural pozzolan and natural perlite in controlling the alkali-silica reaction of cementitious materials, *Case Stud. Constr. Mater.* 17 (2022) e01246, <https://doi.org/10.1016/j.cscm.2022.e01246>.
- [63] H. Maraghchi, M. Maraghchi, F. Rajabipour, C.G. Pantano, Pozzolanic reactivity of recycled glass powder at elevated temperatures: reaction stoichiometry, reaction products and effect of alkali activation, *Cem. Concr. Compos.* 53 (2014) 105–114, <https://doi.org/10.1016/j.cemconcomp.2014.06.015>.
- [64] M.R. Karim, F.I. Chowdhury, H. Zabed, M.R. Saidur, Effect of elevated temperatures on compressive strength and microstructure of cement paste containing palm oil clinker powder, *Constr. Build. Mater.* 183 (2018) 376–383, <https://doi.org/10.1016/j.conbuildmat.2018.06.147>.
- [65] I. Garcia-Lodeiro, P.M. Carmona-Quiroga, R. Zarzuela, M.J. Mosquera, M. T. Blanco-Varela, Chemistry of the interaction between an alkoxysilane-based impregnation treatment and cementitious phases, *Cem. Concr. Res.* 142 (2021) 106351, <https://doi.org/10.1016/j.cemconres.2020.106351>.
- [66] S. Çelikten, M. Saridemir, K. Akçaoğlu, Effect of calcined perlite content on elevated temperature behaviour of alkali activated slag mortars, *J. Build. Eng.* 32 (2020) 101717, <https://doi.org/10.1016/j.jobe.2020.101717>.
- [67] Z. Li, X. Zhou, B. Shen, Fiber-cement extrudates with perlite subjected to high temperatures, *J. Mater. Civ. Eng.* 16 (2004) 221–229, [https://doi.org/10.1061/\(ASCE\)0899-1561\(2004\)16:3\(221\)](https://doi.org/10.1061/(ASCE)0899-1561(2004)16:3(221)).
- [68] I.E. Ariyaratne, A. Ariyanayagam, M. Mahendran, Bushfire-resistant lightweight masonry blocks with expanded perlite aggregate, *Fire* 5 (2022) 132, <https://doi.org/10.3390/fire5050132>.